Applied and Environmental Microbiology, Feb. 2011, p. 1231–1242 Vol. 77, No. 4
0099-2240/11/$12.00 doi:10.1128/AEM.01352-10

Microorganisms with Novel Dissimilatory (Bi)Sulfite Reductase Genes Are Widespread and Part of the Core Microbiota in Low-Sulfate Peatlands▽†

Doris Steger,[1] Cecilia Wentrup,[1]‡ Christina Braunegger,[1] Pinsurang Deevong,[1,2] Manuel Hofer,[1] Andreas Richter,[3] Christian Baranyi,[1] Michael Pester,[1] Michael Wagner,[1] and Alexander Loy[1]*

Department of Microbial Ecology, Vienna Ecology Center, Faculty of Life Sciences, University of Vienna, Althanstrasse 14, A-1090 Vienna, Austria[1]; Department of Microbiology, Faculty of Science, Kasetsart University, 50 Phaholyothin Road, Jatujak, Bangkok 10900, Thailand[2]; and Department of Chemical Ecology & Ecosystems Research, Vienna Ecology Center, Faculty of Life Sciences, University of Vienna, Althanstrasse 14, A-1090 Vienna, Austria[3]

Received 7 June 2010/Accepted 24 November 2010

Peatlands of the Lehstenbach catchment (Germany) house as-yet-unidentified microorganisms with phylogenetically novel variants of the dissimilatory (bi)sulfite reductase genes *dsrAB*. These genes are characteristic of microorganisms that reduce sulfate, sulfite, or some organosulfonates for energy conservation but can also be present in anaerobic syntrophs. However, nothing is currently known regarding the abundance, community dynamics, and biogeography of these *dsrAB*-carrying microorganisms in peatlands. To tackle these issues, soils from a Lehstenbach catchment site (Schlöppnerbrunnen II fen) from different depths were sampled at three time points over a 6-year period to analyze the diversity and distribution of *dsrAB*-containing microorganisms by a newly developed functional gene microarray and quantitative PCR assays. Members of novel, uncultivated *dsrAB* lineages (approximately representing species-level groups) (i) dominated a temporally stable but spatially structured *dsrAB* community and (ii) represented "core" members (up to 1% to 1.7% relative abundance) of the autochthonous microbial community in this fen. In addition, denaturing gradient gel electrophoresis (DGGE)- and clone library-based comparisons of the *dsrAB* diversity in soils from a wet meadow, three bogs, and five fens of various geographic locations (distance of ~1 to 400 km) identified that one *Syntrophobacter*-related and nine novel *dsrAB* lineages are widespread in low-sulfate peatlands. Signatures of biogeography in *dsrB*-based DGGE data were not correlated with geographic distance but could be explained largely by soil pH and wetland type, implying that the distribution of *dsrAB*-carrying microorganisms in wetlands on the scale of a few hundred kilometers is not limited by dispersal but determined by local environmental conditions.

Peatlands contain 15% to 30% of the global soil carbon (13, 79) and represent a net carbon sink that has contributed to global cooling in the past 8,000 to 11,000 years (21). While peatlands are generally resilient to external perturbation, it is predicted that long-term global changes such as warming, decreased precipitation, and increased atmospheric deposition of reactive nitrogen and sulfur compounds will transform peatlands into new ecosystem types, accompanied by unforeseeable changes in the carbon balance (17). The carbon loss from peatlands is mediated largely by the anaerobic microbial decomposition of organic matter to the greenhouse gases carbon dioxide and methane (36), and it is estimated that 10 to 20% of the globally emitted methane is derived from peatlands (30, 87). Primary and secondary fermentation and subsequent methanogenesis are considered to be the main carbon degradation processes because of the absence or limited availability of alternative electron acceptors. However, other microbial processes, such as denitrification and dissimilatory iron and sulfate reduction, can occur together with methanogenesis in the same peat soil fraction and contribute considerably to anaerobic carbon mineralization (4, 5, 43, 44). Fluctuations in environmental conditions on short- and long-term scales govern trophic interdependencies among microorganisms. Transitions between synergistic (e.g., the syntrophic interspecies transfer of hydrogen/formate) and antagonistic (e.g., competition for the same substrates) microbial interactions determine the extent of carbon flow diversion away from methanogenesis. A prime example is the suppression of microorganisms catalyzing methanogenic carbon degradation by sulfate-reducing microorganisms (SRM) that are energetically favored in the competition for substrates such as acetate, alcohols, and hydrogen (22, 81, 82). While sulfate concentrations are generally low in peatlands (10 to 300 μM), ongoing sulfate reduction proceeds at rates (2.5 to 340 nmol cm^{-3} day^{-1}) that are comparable to rates in sulfate-rich environments such as marine sediments (5, 40, 41). It was previously proposed that such high sulfate reduction rates are fueled by an anoxic recycling of reduced sulfur compounds via the so-called "thiosulfate shunt" (5). The alternative replenishment of the sulfate pool by the reoxidation of reduced sulfur species in the presence of oxygen

* Corresponding author. Mailing address: Department of Microbial Ecology, Vienna Ecology Center, Faculty of Life Sciences, University of Vienna, Althanstrasse 14, A-1090 Vienna, Austria. Phone: 43 1 4277 54207. Fax: 43 1 4277 54389. E-mail: loy@microbial-ecology.net.

‡ Present address: Department of Molecular Ecology, Max Planck Institute for Marine Microbiology, Celsiusstr. 1, D-28359 Bremen, Germany.

† Supplemental material for this article may be found at http://aem.asm.org/.

▽ Published ahead of print on 17 December 2010.

is dependent on the vegetation type and alternating periods of precipitation and drought (14, 18, 64, 68, 86). In addition, increasing global atmospheric sulfur pollution and acid precipitation contribute to terrestrial sulfate pools and are predicted to repress methane emissions from peatlands by up to 15% within the first third of this century (22).

Given the significance of dissimilatory sulfate reduction in peatlands, it is surprising that most information about the identity of microorganisms catalyzing this process in peatlands is derived from studies of a single model fen system (Schlöppnerbrunnen) located in the forested Lehstenbach catchment (Bavaria, Germany). Different redox processes such as fermentation (25), methanogenesis (29), denitrification (63), Fe(III) reduction (69), and sulfate reduction (2, 51) are present and have been studied at this site (4). The atmospheric deposition of sulfur originating from the combustion of soft coal in Eastern Europe until the 1990s led to the accumulation of sulfur species in the soils of this catchment. Although air pollution affecting this site has decreased in recent years (39), historically deposited sulfate stored in upland soils can desorb and is then transported via groundwater flow into the fen, where it drives dissimilatory sulfate reduction (1). DNA stable isotope probing using *in situ* concentrations of typical ^{13}C-labeled degradation intermediates (mixture of lactate, acetate, formate, and propionate) has shown that a low-abundance *Desulfosporosinus* species, representing on average only 0.006% of the total bacterial and archaeal 16S rRNA genes, has the potential to be responsible for a substantial part of the sulfate reduction in the studied fen. However, a large fraction of the sulfate reduction observed *in situ* still remains unexplained (67). Other microorganisms that are potentially involved in sulfate reduction were previously detected in this fen by using 16S rRNA gene- and *dsrAB*-based diversity analyses. Few of these *dsrAB* sequences were affiliated with the previously described SRM genera *Desulfomonile* and *Syntrophobacter*, but most of the retrieved *dsrAB* sequences may derive from new taxa, as they represent novel lineages without cultivated representatives (51, 67, 73). Microorganisms that respire sulfite or sulfate anaerobically depend on the *dsrAB*-encoded key enzyme dissimilatory (bi)sulfite reductase for energy conservation, and thus, these genes have been widely used as markers for PCR-based molecular diversity studies of this guild (16, 38, 46, 84). However, some organisms that are phylogenetically related to SRM but that have seemingly lost the ability for sulfite/sulfate reduction can also harbor *dsrAB*. The *dsrAB* sequences of these organosulfonate reducers (45) or syntrophs (32) can be amplified by the commonly used DSR1F-DSR4R PCR primer mix (50). DNA stable isotope probing experiments targeting *dsrAB* in incubations with a mixture of ^{13}C-labeled lactate, acetate, formate, and propionate could therefore not unambiguously link members of the novel *dsrAB* lineages to sulfate reduction in the Schlöppnerbrunnen peatland (67). Besides their unknown identity and ecophysiological function, additional important questions regarding the ecology of these enigmatic *dsrAB*-containing microorganisms remain unanswered: what is their actual abundance in peatlands, are they a stable part of the microbial peatland community or do they occur only sporadically, and are they endemic to the Schlöppnerbrunnen fen site or more widely distributed in different types of wetlands? Using a set of molecular ecology tools, we address these questions in this study and demonstrate that some *dsrAB*-containing microorganisms are widespread in peatlands and can thrive in these systems in considerable numbers.

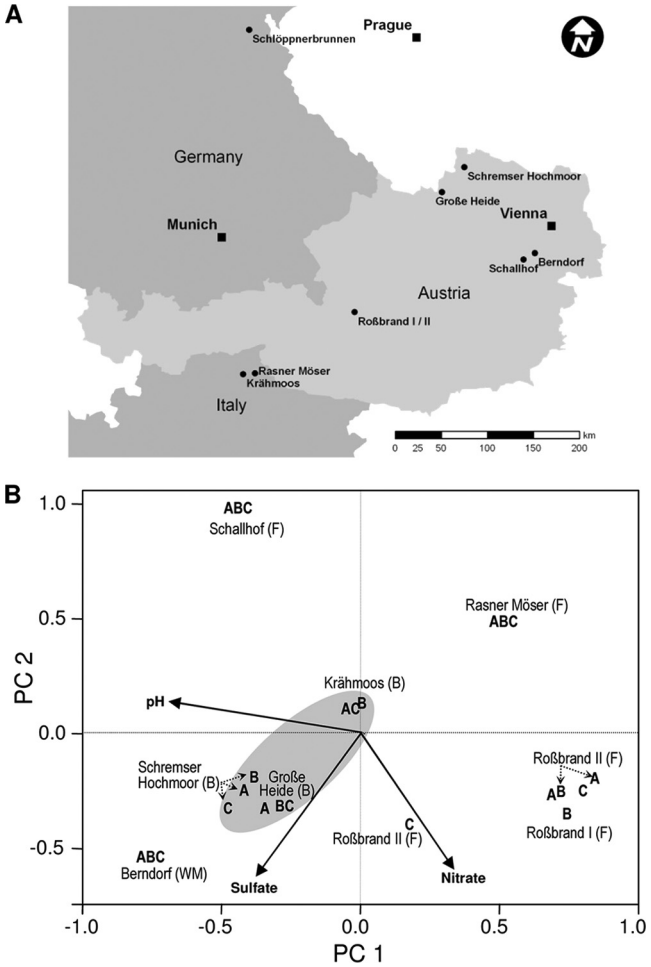

FIG. 1. (A) Geographic locations of the investigated wetlands (filled circles). (B) Projection of the wetland soil samples on the ordination plane formed by PC1 and PC2 from *dsrB* DGGE-based community structure data and relationships of PC1 and PC2 to the pH and the sulfate and nitrate concentrations of soil water (indicated by arrows). For each wetland site, the positions of the three replicate soil cores (indicated by the letters A, B, and C) in the ordination biplot are depicted (positions of the Schremser Hochmoor cores are additionally indicated by arrows with dashed lines). DGGE data from the Schlöppnerbrunnen II fen site were not included in the PC analysis because the corresponding environmental parameters were not determined. The wetland type is indicated: B, bog; F, fen; WM, wet meadow. Gray shading additionally highlights the clustering of bog soil samples. PC1 was strongly negatively correlated with pH (correlation coefficient of −0.9963), whereas PC2 was moderately negatively correlated with sulfate (correlation coefficient of −0.7286) and nitrate (correlation coefficient of −0.6834).

MATERIALS AND METHODS

Description of sites, sampling of soil, and measurement of environmental parameters. The geographic distribution and major characteristics of the nine wetland sites analyzed in this study are summarized in Fig. 1A and Table S1 in the supplemental material. The main sampling site, the acidic lowland fen Schlöppnerbrunnen II (50°08′38″N, 11°51′41″E), is located in the Lehstenbach catchment in the Fichtelgebirge mountains (Bavaria, Germany) at an altitude of

700 m above sea level. Soils are histosols on granite bedrock. This minerotrophic fen has an average peat accumulation of about 50 cm, and its vegetation is dominated by *Carex canescens*, *Carex rostrata*, *Juncus effusus*, *Molinia caerulea*, and *Eriophorum vaginatum* (see references 3, 44, 51, 68, and 69 for information on the biogeochemistry of this fen). Samples collected in 2001 (24 July) were retrieved from a single soil core, which was divided into four depth sections (0 to 7.5, 7.5 to 15, 15 to 22.5, and 22.5 to 30 cm) (51). In 2004 (21 September) and in 2007 (16 May), soil cores (diameter, ~8 cm) were collected from three random locations within the site (the approximate distance between locations was 15 m) and were subsequently divided into four depth sections (0 to 5, 5 to 10, 10 to 15, and 15 to 20 cm). Two additional depth sections (20 to 30 and 30 to 40 cm) were collected in 2007. Besides Schlöppnerbrunnen II, triplicate soil cores (two depth sections, ~0 to 20 and ~20 to 40 cm) were taken from random locations at eight additional wetland sites in Italy and Austria (Fig. 1A and Table S1). Soil water was collected from each 0- to 40-cm core from the eight sites and immediately transported on dry ice to the laboratory for determinations of pH and concentrations of nitrate and sulfate. The soil water pH of each replicate core was analyzed by using a pH meter (WTW inoLab level 1; WTW GmbH, Weilheim, Germany). After pooling the soil water samples from the three replicate cores, sulfate and nitrate concentrations were determined by ion chromatography as described previously (31). Immediately at the sampling site, samples for molecular analyses were homogenized, frozen on dry ice for transportation, and stored at −80°C upon arrival at the laboratory.

DNA extraction. For microarray, quantitative PCR (qPCR), and denaturing gradient gel electrophoresis (DGGE) analyses, DNA was extracted from approximately 250 mg (wet weight) of each soil sample using the Power Soil DNA kit (MoBio Laboratories, Solana Beach, CA).

Fluorescence labeling of target genes for microarray hybridization. A previously reported protocol (6) was adapted for the fluorescence labeling of *dsrAB* amplicons. Initially, an approximately 1.9-kb fragment of *dsrAB* was PCR amplified from 5 ng reference clone DNA or 50 ng environmental DNA using the degenerate primers DSR1Fmix (equimolar mixture of 10 μM each DSR1F variant) and DSR4Rmix (equimolar mixture of 10 μM each DSR4R variant) (see Table S2 in the supplemental material). 16S rRNA and nucleotide transport protein (*ntt*) reference genes, targeted by control probes, were amplified by the primer pairs listed in Table S3 in the supplemental material (50 μM each primer). All forward primers contained a T3 promoter site sequence (5′-AATT AACCCTCACTAAAGGG-3′) at the 5′ end to enable T3 RNA polymerase-based transcription labeling of the PCR products. PCR mixtures (50 μl) were prepared by using 2 mM each deoxynucleoside triphosphate, 10× *Taq* buffer, 2 mM $MgCl_2$, and 2 U of *Taq* DNA polymerase (Fermentas Inc., Hanover, MD). For the amplification of environmental samples, 1 μl of bovine serum albumin (20 μg/μl; New England BioLabs Inc., Beverly, MA) was additionally added to each reaction mixture to enhance PCR efficiency. Reference and control genes were amplified by using an initial denaturation step at 95°C for 3 min, followed by 30 cycles of denaturation at 95°C for 30 s; annealing at 48°C (*dsrAB*), 52°C (16S rRNA gene), or 55°C (*ntt*) for 30 s; and elongation at 72°C for 1 min 10 s. The cycling was completed by a final elongation step at 72°C for 3 min. PCR amplification of *dsrAB* from environmental DNA extracts was carried out by two successive hot-start PCRs (i.e., the addition of the template DNA to the final PCR mix at 96°C) to minimize unspecific amplification products (12). The first PCR was performed in touchdown mode by using an initial denaturation step at 95°C for 3 min, followed by 10 cycles of denaturation at 95°C for 30 s, annealing at 58°C to 48°C for 30 s (after each cycle, the temperature was reduced by 1°C), and elongation at 72°C for 1 min 10 s. Ten additional PCR cycles at a constant annealing temperature of 48°C were performed prior to the final elongation step at 72°C for 3 min. PCR products were examined by 1% agarose gel electrophoresis for the presence and sizes of amplicons. PCR products were purified from the gel by using the Montage DNA gel extraction kit (Millipore, Bedford, MA) according to the manufacturer's instructions. One microliter of purified PCR product was reamplified in a second PCR applying an initial denaturation step at 95°C for 3 min, followed by 20 cycles of denaturation at 95°C for 30 s, annealing at 48°C for 30 s, and elongation at 72°C for 1 min 10 s. The cycling was completed by a final elongation step at 72°C for 3 min. PCR products were purified by using the QIAquick PCR purification kit (Qiagen, Hilden, Germany).

Target labeling was achieved by *in vitro* transcription according to the following protocol. A solution containing 500 ng of purified PCR product; 4 μl 5× T3 RNA polymerase buffer (Fermentas); 2 μl dithiothreitol (100 mM); 0.5 μl RNasin (40 U/μl) (Promega GmbH, Mannheim, Germany); 1 μl each of ATP, CTP, and GTP (each 10 mM); 0.5 μl UTP (10 mM); 2 μl T3 RNA polymerase (20 U/μl) (Fermentas); and 0.75 μl Cy3-UTP (5 mM) was adjusted with RNase-free water to a total volume of 20 μl and incubated at 37°C for 4 h. The DNA template was subsequently degraded by the addition of 2 U DNase I (Fermentas) and incubation at 37°C for 15 min. Enzymatic digestion was stopped with 2 μl of EDTA (25 mM; Fermentas). Following an adjustment of the volume to 100 μl with Tris-EDTA (TE) buffer (10 mM Tris-HCl [pH 7.5], 1 mM EDTA), RNA was precipitated with 10 μl of 5 M NaCl and 300 μl of ethanol. RNA was washed with 500 μl of ice-cold 70% ethanol and resuspended in 50 μl TE buffer. The RNA concentration and the amount of incorporated dye were measured with an ND-1000 spectrophotometer (Nanodrop Inc.). Labeled RNA was fragmented by incubation with 10 mM $ZnCl_2$ and 20 mM Tris-HCl (pH 7.4) at 60°C for 30 min. Fragmentation was stopped by the addition of 10 mM EDTA (pH 8.0). Labeled RNA was divided into several aliquots that were stored at −20°C.

Probe design and manufacturing of microarrays. Probes targeting *dsrA* or *dsrB* were designed by using the probe tools of the ARB software package (53) and a *dsrAB* ARB database containing approximately 500 sequences (>1,500 nucleotides) from pure cultures (50, 89) and environmental studies. Based on a distance matrix tree of all previously reported *dsrAB* clone sequences retrieved from the Schlöppnerbrunnen I+II system (51, 73), 146 probes with an average length of 30 bases were designed to target different clone groups from the study site (see Fig. S1 and Table S4 in the supplemental material). The thermodynamic properties of the probes were calculated by using the two-state hybridization server of DINAMelt (default settings were linear DNA, 37°C, 1 M Na^+, 0 M Mg^{2+}, and a 0.1 mM strand concentration) (54). Probe lengths were adjusted to obtain similar theoretical free-energy (Gibbs free energy [deltaG]) values. The final probes had a length of 27 to 34 nucleotides with an average deltaG of −41.0 ± 0.7 kcal/mol (Table S4). The *in silico* specificity and number of weighted mismatches to nontarget *dsrAB* sequences of each probe were determined by using probeCheck (48). Oligonucleotides for microarray spotting were synthesized by Microsynth (Balgach, Switzerland). The 5′ end of each oligonucleotide probe carried a T spacer consisting of 30 dTTP molecules, and the 5′-terminal dTTP was aminated to allow the covalent coupling of the oligonucleotides to aldehyde group-coated VSS-25 glass slides (CEL Associates, Houston, TX). Each probe was adjusted to a concentration of 50 pmol/μl in 50% dimethyl sulfoxide and printed onto the slide by using a BioRobotics MicroGrid spotter (Genomics Solutions, Ann Arbor, MI) under conditions of constant temperature (20°C) and humidity (minimum, 50%) conditions. Each microarray contained three and six replicate spots of each *dsrAB*-targeted probe and control probe, respectively. Freshly spotted DNA microarrays were incubated overnight at room temperature in a humid chamber. Slides were further treated with sodium borohydride as described previously (52).

Microarray hybridization. Eighty nanograms (for clones) and 500 ng (for environmental samples) of labeled *dsrAB* RNA fragments and defined amounts of labeled RNA targeting the control probes (see Table S3 in the supplemental material) were mixed with 120 μl of hybridization buffer (0.1% SDS, 0.1% 100× Denhardt's reagent [Invitrogen], 6× SSC [1× SSC is 0.15 M NaCl plus 0.015 M sodium citrate], and 15% formamide) and incubated at 65°C for 5 to 15 min prior to hybridization. A ThermoTWISTER incubator (Quantifoil Instruments GmbH, Jena, Germany) and a HybriWell HBW2222-FL sealing system (Grace BioLabs) were used for hybridization. Microarrays were hybridized for 17 h at 55°C under continuous shaking at 400 rpm. Following hybridization, slides were washed by shaking at room temperature for 5 min in 2× SSC–0.1% SDS, for 5 min in 0.1× SSC, and finally for 20 s in ice-cold double-distilled water. Slides were dried by centrifugation (3 min at 300 × *g*), stored at room temperature in the dark, and scanned the same day.

Scanning and data analysis. Fluorescence images were recorded by scanning the slides at a 10-μm resolution with a GenePix Personal 4100A array scanner (Axon Instruments, Molecular Devices Corporation, Sunnyvale, CA). Each pixel line of the selected area was scanned three times, and the obtained signals were averaged to generate the fluorescence image. The gain of the photo multiplier tube was adjusted to record images with signal intensities just below the saturation level. Scanned images were saved as multilayer tiff images and were analyzed with GenePix Pro 6.0 software (Axon Instruments). Low-quality hybridizations were repeated.

Microarray hybridization results were first corrected for differences in the local background according to the formula $SBR_{Pi} = S_{Pi} \times B_{Pi}^{-1}$, where SBR_{Pi} is the signal-to-noise ratio of the probe spot *Pi*, S_{Pi} is the median pixel intensity of the specific probe spot, and B_{Pi} is the median pixel intensity of the local background area around probe *Pi*. To account for variations between different hybridizations, the mean signal-to-noise ratio, $\bar{x}\ SBR_{Ci}$, of 10 internal control oligonucleotides (dsrCONT1 to dsrCONT4 and dsrCONT7 to dsrCONT12) and differences in labeling efficiency were used to normalize the SBR_{Pi} value by using the formula $nSBR_{Pi} = (SBR_{Pi} \times \bar{x}\ SBR_{ci}^{-1}) \times [\text{dye}]^{-1} \times [\text{template}] \times 100$, where $nSBR_{Pi}$ is the normalized signal-to-noise ratio of the probe spot *Pi*, [dye] is the concentration of incorporated Cy3 dye molecules in pmol/μl, and [template] is the concentration of labeled RNA in ng/μl.

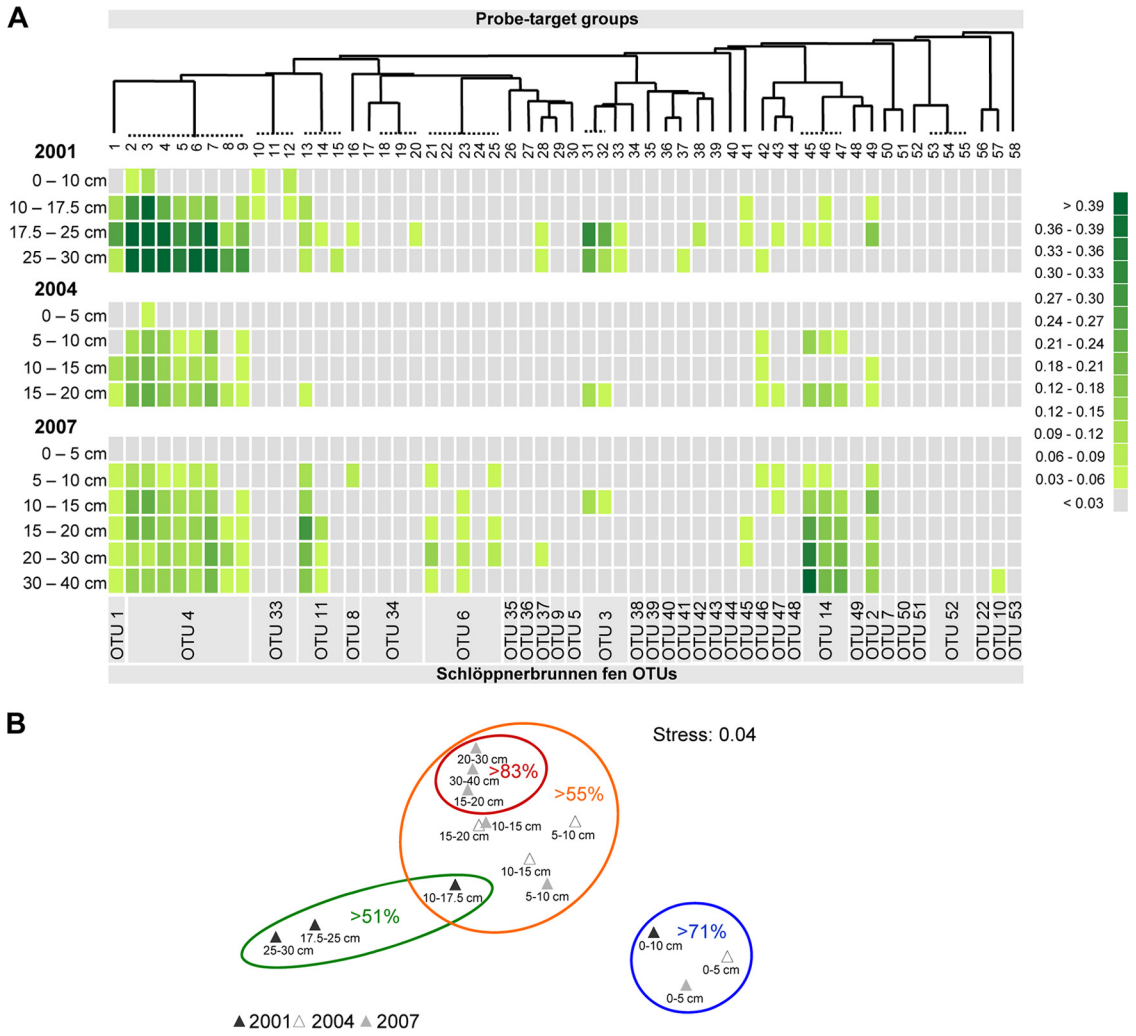

FIG. 2. Microarray-based *dsrAB* diversity analysis of Schlöppnerbrunnen II fen soils sampled from different depths in the years 2001, 2004, and 2007. (A) Results of microarray hybridizations are displayed as mean nSBRs of all probes within a probe-target group and are averaged between triplicate hybridizations (technical replicates for the year 2001 and biological replicates for the years 2004 and 2007) (results of individual replicate analyses are presented in Fig. S2 in the supplemental material). The color code translates into different mean nSBR values (right-axis legend). Sampling depth and year values are shown on the left axis. Probe-target groups are arranged phylogenetically on the upper horizontal axis according to their position in a schematic *dsrAB* neighbor-joining tree. The affiliation of probe-target groups to previously detected Schlöppnerbrunnen fen OTUs (51, 73) is indicated on the lower horizontal axis. Figure S1 and Table S4 in the supplemental material include further information on the phylogeny and GenBank accession numbers of the clones affiliated with the different probe-target groups and OTUs. (B) Multidimensional scaling plot based on Bray-Curtis similarities between microarray hybridization patterns shown in A. Minimal Bray-Curtis similarities of all samples in a given group of samples are indicated in color.

Heat maps of the microarray results were generated by using the software visualization tool JColorGrid (33). Nonmetric multidimensional scaling ordinations based on Bray-Curtis similarities between microarray results (based on the mean normalized signal-to-background ratios [nSBRs] of all probes in the respective probe-target groups) (Fig. 2A) were performed by using PRIMER 5 software (10).

Quantitative real-time PCR. qPCR assays were performed by using an iCycler IQ thermocycler (Bio-Rad Laboratories GmbH, München, Germany) and Platinum SYBR green qPCR Super Mix-UDG (Invitrogen Corporation, Carlsbad, CA) according to the manufacturer's instructions. 16S rRNA gene- and *dsrA*-targeted primers were designed by using the "probe design" and "probe match" tools of the ARB program package. The potential formation of primer dimers and theoretical melting temperatures were determined by using the open-source program Primer3 (70) and the oligonucleotide property calculator OligoCalc (37), respectively. Primers, assay performances, and cycling conditions are given in Tables 1 and 2. Thermal cycling was initiated by a denaturation step at 94°C for 3 min, followed by 40 to 45 cycles of denaturation at 94°C for 40 s, annealing at the specific temperature for 40 s, and elongation at 72°C for 40 to 45 s. PCR products were used as standards for assay calibration and were amplified from the cloned sequences given in Table 1. The specific annealing temperature for each primer pair was determined by gradient PCR using perfectly matching target genes and a selection of nontarget clones with mismatches in the primer target site as templates. For each PCR product, a single band of the expected size was observed by agarose gel electrophoresis. Five nanograms of soil DNA was used as a template per PCR. The specificity of each qPCR assay was confirmed by melting-curve analyses of the sample-derived and respective reference clone-derived PCR products. Additionally, environmental PCR products were cloned, and the identities of a few selected clones were verified by sequencing. The absence of PCR-inhibitory substances was confirmed by qPCR analyses (using primers 1389F and 1492R) of dilution series of five selected soil DNA extracts, showing efficiencies and correlation coefficients similar to those of the standards.

Denaturing gradient gel electrophoresis. Triplicate soil cores from nine different wetlands (including Schlöppnerbrunnen II fen samples taken in 2004) were analyzed by using newly developed forward primers for *dsrB*-based DGGE.

TABLE 1. Primers used for quantitative real-time PCR

Primer	Sequence (5′–3′)	Length (bp)	%GC content	Target gene	Target group	Reference
DsrA243Fb	CAC GAC CAC CGA TCA GCT	18	61	*dsrA*	OTU 2	This study
DsrA561Rb	GTA CTT GGT CAS TTC GGC C	19	58			
DsrA243Fa	CAC CAC CAC CGA TGA ACT	18	56	*dsrA*	OTU 1	This study
DsrA561Ra	ATA GGC CTT BAC YGC GGC C	19	58–68			
DsrA216F	CTC AAC GGG AGA CAT CGT T	19	53	*dsrA*	OTU 6	This study
DsrA561Re	ATA GGC TTT GAC CGC TGC C	19	58			
SYBAC836F	GGG TAC TCA TTC CTG CTG TG	20	55	16S rRNA	*Syntrophobacter* spp. and related bacteria	This study
SYBAC986R	CCG GGG ATG TCA AGC CCA	18	67			
1389F	TG TAC ACA CCG CCC GT	16	63	16S rRNA	*Bacteria* and *Archaea*	67
1492R	GGY TAC CTT GTT ACG ACT T	16	44–50			

DNA extracts obtained from the different depth fractions of one soil core were pooled prior to PCR. The preparation of GC-clamp-tagged *dsrB* amplicons was carried out by using a nested PCR approach. First, *dsrAB* fragments were amplified from 20 ng soil DNA in technical duplicates using the degenerate primers DSR1Fmix and DSR4Rmix (see Table S2 in the supplemental material) for hot-start touchdown PCR as described above, except that only 20 cycles (10 cycles with annealing at 58°C to 48°C, followed by 10 cycles at 48°C) were performed. The *dsrAB* amplicons of duplicate PCRs were mixed, purified by gel electrophoresis using the Montage DNA gel extraction kit (Millipore), and used as a template for the *dsrB*-targeted PCR. Five separate PCRs per template were performed by using the degenerate primers DSR4Rmix (10 μM each variant) and GC-clamp-carrying DSR1728F mixes A to E (Table S5). Reaction mixes (total volume, 100 μl) were prepared with 2 mM each deoxynucleoside triphosphate, 10× *Taq* buffer, 2 mM $MgCl_2$, 2 U of *Taq* DNA polymerase (Fermentas), 2 μl of bovine serum albumin (20 mg/ml; New England BioLabs), and 2 μl of template. Amplification was started by an initial denaturation step at 95°C for 3 min, followed by 20 cycles of denaturation at 95°C for 30 s, annealing at 55°C for 30 s, and elongation at 72°C for 20 s. Cycling was completed by a final elongation step at 72°C for 3 min. Successfully amplified PCR products of each sample were pooled and concentrated to ~50 μl by using a vacuum centrifuge. Additionally, three *dsrAB* plasmids were subjected to the procedure described above and used as an internal standard to allow comparisons between DGGE gels. DGGE was performed as described previously (59). In brief, a denaturing gradient of 30 to 80% denaturants (100% denaturant mixture consisting of 7 M urea and 40% formamide) was used in an 8% (wt/vol) polyacrylamide gel. DGGE was performed with 1× Tris-acetate-EDTA buffer at 60°C and at a voltage of 150 V for 6 h. Following electrophoresis, the gels were incubated for 60 min in a SYBR green I solution. For identification, individual bands were excised, reamplified, purified using the QIAquick PCR purification kit (Qiagen), and sequenced directly.

A principal component (PC) analysis (Canoco for Windows 4.5) (76) was performed by using presence and absence data for DGGE bands and *z*-transformed environmental variables (i.e., pH, sulfate, and nitrate). Data for Schlöppnerbrunnen II were excluded from this analysis, as corresponding environmental parameters were not determined for these samples. In addition, two separate Bray-Curtis similarity matrices were calculated by using the DGGE band presence and absence data and the environmental parameters. A geographical distance matrix was generated based on the air-line distances (in km) between sampling sites. The three matrices were tested pairwise for similar patterns by using the RELATE routine of the Primer 5 program (10) (999 permutations; Spearman's rho).

Clone library construction and comparative sequence analysis. A *dsrAB* clone library was constructed from pooled DNA extracts of all Rasner Möser fen soil subsamples using the degenerate primers DSR1Fmix and DSR4Rmix (see Table S2 in the supplemental material). Touchdown PCR was performed as described above, with the exception that 25 cycles (10 cycles with annealing at 58°C to 48°C, followed by 15 cycles at 48°C) were conducted. The cycling was completed by a final elongation step at 72°C for 10 min. The presence and sizes of the amplification products were determined by agarose (1%) gel electrophoresis. Prior to cloning using the TOPO XL cloning kit (Invitrogen), PCR products were purified from the gel by using the Montage DNA gel extraction kit (Millipore).

Phylogenetic analyses were performed by using distance matrix, maximum parsimony, and maximum likelihood methods implemented in the ARB program package (53). DOTUR (72) was used to group deduced DsrAB and DsrA amino acid sequences from Schlöppnerbrunnen fen soil microorganisms in operational taxonomic units (OTUs) based on an identity threshold of 90% (approximately

TABLE 2. Assay performances and cycling conditions of primers used for quantitative real-time PCR

Primer	Annealing temp (°C)	Primer concn (nM)	Approximate length of PCR product (bp)	Standard templates (GenBank accession numbers)	qPCR performance		
					Mean efficiency (%) ± SD	Linearity R^2	Dynamic range (no. of target genes/PCR)
DsrA243Fb DsrA561Rb	64	250	330	AY167467, AY167479, AY167468	83.2 ± 3.0	0.98	10^2–10^6
DsrA243Fa DsrA561Ra	64	250	330	AY167473, AY167466, AY167480	89.8 ± 0.4	0.99	10^2–10^5
DsrA216F DsrA561Re	64	250	360	AY167478, AY167465	73.6 ± 1.4	0.98	10^2–10^6
SYBAC836F SYBAC986R	64	250	160	X70905, X70906	77.5 ± 0.1	0.99	10^2–10^6
1389F 1492R	52	750 1,000	120	X70905, X70906	90.0 ± 2.8	1.00	10^2–10^6

defining species-level groups [38, 51]). The same was done separately for DsrB sequences obtained in the DGGE analysis. Coverage was calculated according to a method described previously by Good (24). Phylogenetic analyses were performed by using an indel filter (543 valid alignment positions after the exclusion of variable regions with insertions and deletions). A consensus tree was drawn based on PHYLIP ProML (JTT), protein parsimony, and distance matrix (FITCH, JTT, global rearrangements, and randomized input order of sequences) analyses of sequences of >500 amino acids. Sequences of <500 amino acids were individually added to the trees without changing the overall topology by use of the ARB parsimony interactive method.

Accession numbers. The sequences determined in this study have been deposited in the GenBank database under accession numbers GU127936 to GU127971 (*dsrAB*) and GU127876 to GU127935 (*dsrB*). The microarray data have been deposited in the NIH National Center for Biotechnology Information Gene Expression Omnibus (GEO) database (www.ncbi.nlm.nih.gov/geo/) under accession number GSE24582.

RESULTS

Development of a Schlöppnerbrunnen fen-specific *dsrAB* functional gene array. A habitat-specific functional gene array (FGA) was designed and optimized for a parallel diversity analysis of *dsrAB*-containing microorganisms in the Schlöppnerbrunnen fen system. In contrast to more-universal FGAs that consist of thousands of probes, such as the GeoChip (26), this low-density, Schlöppnerbrunnen fen-specific *dsrAB* FGA has the advantage that the specificity of almost every probe on the microarray can be empirically evaluated by using appropriate reference target sequences. This FGA covers all *dsrAB* and *dsrA* sequences from the Schlöppnerbrunnen fen system known at the time of microarray design, comprising 34 of 53 currently known Schlöppnerbrunnen fen OTUs (each OTU comprises sequences with at least 90% amino acid identity) (51, 67, 73). These 34 Schlöppnerbrunnen fen OTUs were targeted by 146 oligonucleotide probes that detect 58 groups of *dsrAB* sequences according to the multiple-probe concept (49, 85) (see Fig. S1 and Table S4 in the supplemental material). In a first step, hybridization conditions were optimized by performing a series of hybridizations with *dsrAB* reference clone dsrSBI-3 (GenBank accession number AY167467) at increasing formamide concentrations (0 to 60%, at 5% increments) in the hybridization buffer. A formamide concentration of 15% was selected for all subsequent hybridizations as the best compromise between sensitivity (i.e., high signal intensity of perfectly matched probes) and specificity (i.e., high signal intensity ratios between perfectly matched and mismatched probes) (data not shown). In the second step, the specificity of the *dsrAB* FGA was further evaluated by individual hybridization with 36 *dsrAB* reference clones. This set of reference clones contained at least one perfectly matched target for 120 probes. Twenty-six probes could not be fully tested because perfectly matching reference clones were not available. Probe signals with a normalized signal-to-background ratio (nSBR) of equal to or greater than 0.04 were considered positive. Ninety-eight of the 120 tested probes gave a positive signal only with the perfectly matching target clone. False-positive hybridizations occurred only between probes and nontarget sequences with fewer than 2 weighted mismatches. Two probes (dsrB40 and dsrA127) gave false-negative results and were thus excluded from further analyses. In summary, only 0.57% and 0.04% of the 5,256 individual probe-target hybridizations were false positive and false negative, respectively (Table S6). The nSBRs of perfectly matched probe-target duplexes of the final probe set ranged from 0.04 to 2.2 (factor of 55), showing that the signal intensities of individual probes varied considerably. In the third step, the sensitivity of the *dsrAB* FGA was assessed by a series of hybridizations containing different concentrations of the clone dsrSBI-36 (accession number AY167469). One copy, 10 copies, 100 copies, 1,000 copies, 10,000 copies, and 100,000 copies of the respective plasmid were added to 60-ng aliquots (corresponding to approximately 1×10^7 microbial genomes, assuming an average genome size of 5 Mbp) of fen soil DNA (sampled in 2007; depth, 15 to 20 cm) prior to PCR amplification and further target preparation. A minimum of 1,000 plasmids was required for the positive detection of clone dsrSBI-36 by *dsrAB* FGA hybridization. Given that most *dsrAB*-containing microorganisms have only a single copy of *dsrAB* in their genomes, this corresponds to a detection limit of 0.01% of the total microbial community for this target organism (nSBR values of probes targeting clone dsrSBI-36 ranged from 0.17 to 0.41 in the specificity test). Additionally, the spot-to-spot variability (from triplicate spots of the same slide) and the slide-to-slide variability (from replicate spots of different slides) were determined to evaluate the robustness of the microarray analysis. The spot-to-spot variabilities of five randomly chosen arrays, given as mean coefficients of variation of SBR values, were 3.8% ± 0.7% between triplicate spots on a given slide and 7.4% ± 3.7% between spots on three separate slides hybridized with the same fluorescently labeled target RNA. The technical variability of environmental microarray analyses, as determined by hybridizations with labeled RNA prepared from the same environmental sample (in the year 2001; depth, 0 to 10 cm) but from separate DNA extractions and labeling reactions, showed a mean coefficient of variation of 15.3% based on nSBR values. This variability includes the composite methodological biases introduced by DNA extraction, PCR, labeling, and microarray hybridization and lies in the range observed for other previously reported microarray experiments (9, 71, 80).

Temporal and spatial dynamics of *dsrAB*-carrying microorganisms in the Schlöppnerbrunnen II fen. The newly developed Schlöppnerbrunnen fen-specific *dsrAB* FGA was applied to analyze the spatial and temporal distribution of *dsrAB* at the Schlöppnerbrunnen II site. Microarray analyses of soil samples obtained from different depths (0 to 40 cm) were performed in technical triplicates (i.e., analysis of three separate DNA extracts obtained from the same soil core) for the year 2001 and in biological triplicates (i.e., analysis of three different soil cores) for the years 2004 and 2007. Microarray procedures for target preparation, hybridization, and data analysis were kept identical for all soil samples to allow comparisons between different hybridizations. Soil depth profiles of *dsrAB* FGA hybridization patterns that were obtained for the 3 years were generally similar (Fig. 2A), with an average Bray-Curtis similarity of 59% ± 18% among all samples. However, in deeper soil layers, the *dsrAB* diversity was considerably greater than that in the top soil layer, where only a few probe-target groups were detected by the FGA. In accordance with this observation, multidimensional scaling analysis of Bray-Curtis similarities between microarray hybridization patterns clearly separated the top soil layers from all other samples (Fig. 2B).

Members of the novel *dsrAB* OTUs 1 and 4 (51), which are only distantly related to *Desulfobacca acetoxidans* (DsrAB

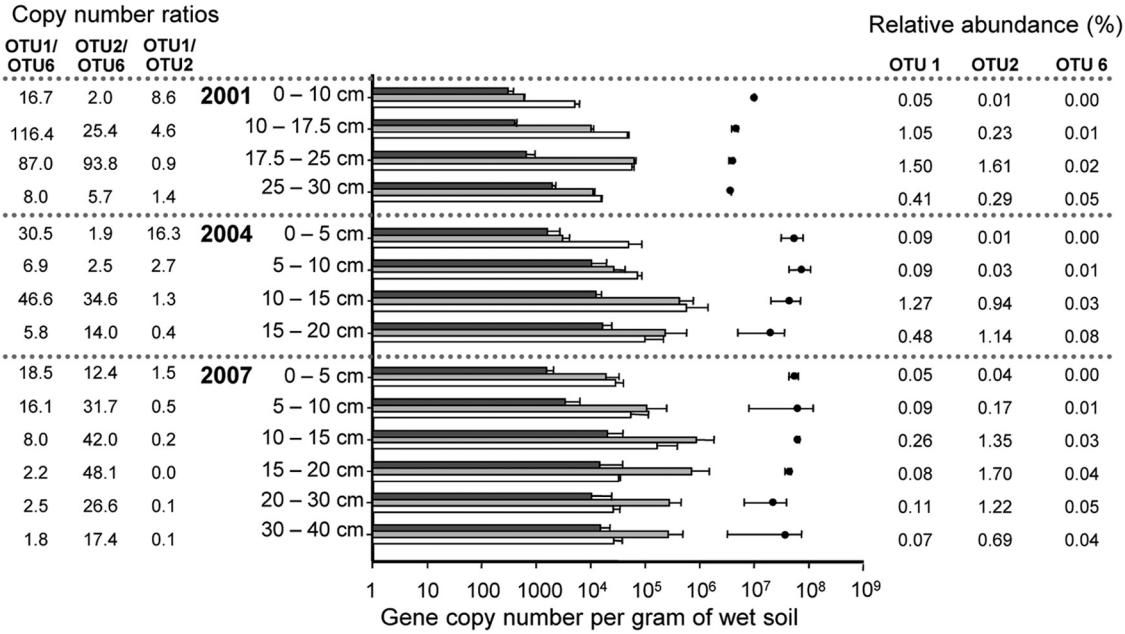

FIG. 3. Absolute and relative abundances of three *dsrAB* OTUs at different depths of the Schlöppnerbrunnen II fen site in the years 2001, 2004, and 2007, as determined by qPCR. Error bars are the standard deviations of the means for the three replicates. Black circles indicate total numbers of bacterial and archaeal 16S rRNA genes. Copy numbers of *dsrA* genes of OTUs 1, 2, and 6 are displayed as white, light gray, and dark gray bars, respectively. Additionally, the relative abundance of each *dsrAB* OTU (given as a percentage of the total number of bacterial and archaeal 16S rRNA genes) and copy number ratios between individual *dsrAB* OTUs are shown for all years and depths.

identities of 69 to 77%), were present in most deeper soil fractions and dominated throughout the analyzed time period, as indicated by positive probe signals for probe-target groups 1 and 2 to 9, respectively. A similar situation was observed for members of the novel *dsrAB* OTUs 2 and 14, with no cultivated close relatives, as indicated by positive probe signals for probe-target groups 49 and 45 to 47, respectively. In addition, the following *dsrAB* groups with no cultivated close relatives were detected frequently in some of the deeper soil layers: members of OTU 3 and OTU 11 and, to a lesser extent, OTUs 45, 46, and 47. Microorganisms related to the genera *Desulfomonile* (OTU 37) and *Syntrophobacter* (OTU 6) were only occasionally detected by *dsrAB* FGA analysis.

To confirm the microarray results, *dsrA*-targeted qPCR assays for OTU 1 (probe-target group 1), OTU 2 (probe-target group 49), and OTU 6 (probe-target groups 21, 23, and 25) were developed and applied to determine the abundance of these OTUs in the Schlöppnerbrunnen II soil samples. Comparisons of *dsrA* copy numbers to the nSBR of the corresponding probe-target groups of the *dsrAB* FGA demonstrated a significant correlation ($P < 0.01$) between qPCR and microarray data, with Pearson coefficients of 0.811 for OTU 1 (with probe-target group 1), 0.756 for OTU 2 (with probe-target group 49), and 0.734 (with probe-target group 21) and 0.863 (with probe-target group 23) for OTU 6. Thus, the qPCR results generally confirmed the microarray results, but, as expected, qPCR assays were also more sensitive than the FGA analysis (Fig. 2A and 3). The average total number of bacterial and archaeal 16S rRNA genes for all samples from different soil depths and years was $3.6 \times 10^7 \pm 1.6 \times 10^7$ copies per gram of wet soil, with total numbers being slightly higher in upper soil layers (Fig. 3). In contrast, *dsrA* copy numbers of all three target OTUs were lowest in the top soil layers and generally increased with soil depth, although OTU 1 and OTU 2 were represented by slightly lower *dsrA* copy numbers in the deepest soil layers. The mean *dsrA* copy numbers per g fen soil were $8.9 \times 10^4 \pm 0.6 \times 10^4$ for OTU 1, $2.1 \times 10^5 \pm 0.07 \times 10^5$ for OTU 2, and $7.9 \times 10^3 \pm 0.6 \times 10^3$ for OTU 6. For all years and soil depths, *dsrA* of the novel OTUs 1 and 2 outnumbered *dsrA* of the *Syntrophobacter*-related OTU 6, with ratios ranging from 1.8 to 116.4 for OTU 1 and from 1.9 to 93.8 for OTU 2 (Fig. 3). The highest relative abundances of OTUs 1 and 2 that were observed for some soil depths ranged from 1% to 1.7% of the prokaryotic community (i.e., percent ratios of *dsrA* copy numbers to total bacterial and archaeal 16S rRNA gene copy numbers). In contrast, the relative abundance of OTU 6 never exceeded 0.08% over the analyzed period (Fig. 3). The mean relative abundances of OTUs 1, 2, and 6 (averaged over soil depth for each sampling time point) ranged from 0.11% to 0.75%, 0.53% to 0.86%, and 0.02% to 0.03%, respectively.

For *Syntrophobacter*-related bacteria (represented by OTU 6), an additional 16S rRNA gene-targeted qPCR assay was developed based on previously reported 16S rRNA gene clone sequences from the Schlöppnerbrunnen fen (51). As expected, 16S rRNA gene- and *dsrA*-based qPCR data for the *Syntrophobacter*-related target group showed a high correlation (Pearson correlation coefficient of 0.854; $P < 0.01$), confirming that *dsrAB* of OTU 6 was indeed derived from *Syntrophobacter*-related bacteria in the Schlöppnerbrunnen fen soil samples (data not shown).

Diversity and biogeography of *dsrAB* in geographically separated wetlands. In order to evaluate whether the *dsrAB*-con-

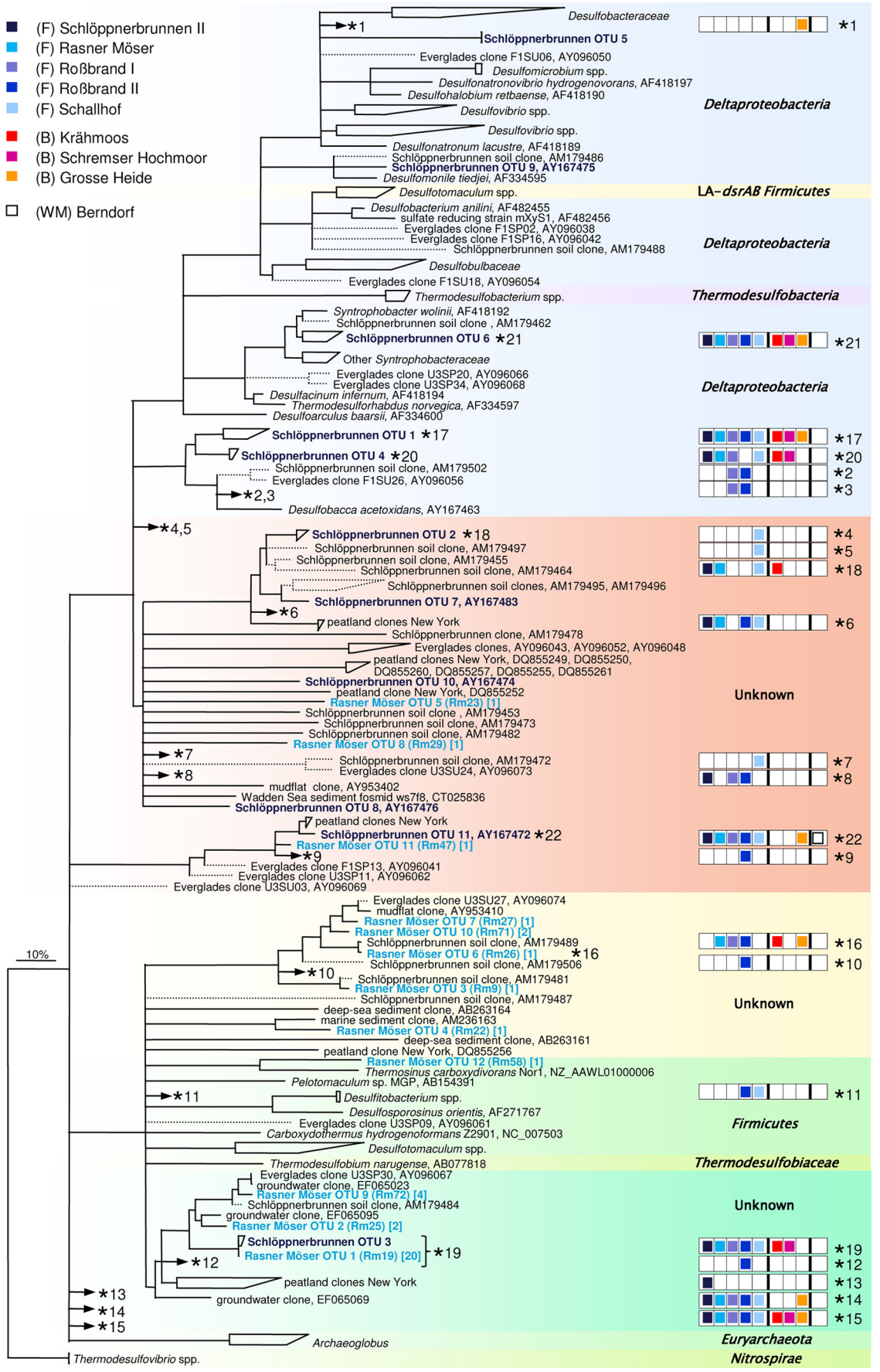

taining microorganisms in the Schlöppnerbrunnen fens are endemic or show a wider geographic distribution, a modified DGGE assay was applied for the fingerprinting of *dsrB* in nine wetlands located in Austria, Italy, and Germany (Fig. 1A, and see Table S1 in the supplemental material). Because the original DGGE forward primer DSRp2060F (23) covers only 29% of all sequences in the *dsrAB* database, we developed a new DSR1728F primer mix, which has a significantly improved *in silico* coverage of 95% (Table S5). This modified *dsrB* DGGE analysis yielded 11 to 40 bands for the different wetland soil samples (Fig. S3). The lowest and highest numbers of DGGE bands were detected in the Berndorf wet meadow soil and the Roßbrand II fen soil, respectively. With the exception of Roßbrand peats I and II, located at a close distance (~1 km) to each other, the *dsrB* DGGE profiles between replicate soil cores were more similar to each other than were *dsrB* DGGE profiles between different wetland sites (Fig. 1B). In addition, all precipitation-fed bogs showed greater similarity in *dsrB* DGGE banding patterns to each other than to other wetland sites. Principal component (PC) analysis resulted in four PCs that together explained 74.1% of the DGGE-based community composition data, with the first two ordination axes (Fig. 1B) accounting for 48.8% of the variation. Correlation analysis between principal components and environmental factors revealed that PC1 was strongly negatively correlated with pH (correlation coefficient of −0.9963), whereas PC2 was moderately negatively correlated with sulfate (correlation coefficient of −0.7286) and nitrate (correlation coefficient of −0.6834). These measured environmental factors explained significantly the differences in the *dsrB* DGGE profiles of the investigated wetlands ($\sigma = 0.568$; $P < 0.001$), whereas there was no major relationship based on the geographical position of the investigated peatlands.

To identify the *dsrAB*-carrying microorganisms in the different peatlands, 160 individual *dsrB* DGGE bands were extracted from the gels, reamplified, and sequenced. Unambiguous *dsrB* sequences were obtained from 59 DGGE bands and grouped into 22 DsrB OTUs (Fig. 4, and see Table S7 in the supplemental material). As observed previously for *dsrAB* sequences from the Schlöppnerbrunnen fen system (51, 73), few OTUs were closely affiliated with representatives of characterized SRM. Ten OTUs, including six previously recovered Schlöppnerbrunnen DsrAB OTUs, were present in at least four out of eight peatlands. Nine OTUs of these widely distributed OTUs were present at bog and fen sites, while *dsrB* DGGE OTU 6 was detected only in fens.

Soil samples from the groundwater-fed fen site Rasner Möser were additionally subjected to a *dsrAB* clone library analysis. A total of 36 partially sequenced *dsrAB* clones (860 to 1,070 bp) formed 12 Rasner Möser OTUs (see Table S8 in the supplemental material), resulting in a Good's coverage of 78%. The *dsrAB* insert of 1 clone per OTU was fully sequenced (~1,900 bp) and analyzed phylogenetically. Only Rasner Möser OTU 12 was moderately related to *Thermosinus carboxydivorans*, while the remaining OTUs had no cultivated close relative (Fig. 4). Rasner Möser OTU 1 (represented by more than half of the *dsrAB* sequences; $n = 20$) and OTU 11 were most closely related to the deep-branching Schlöppnerbrunnen OTU 3 (88.2% to 97.3% amino acid identities) and 11 (90% amino acid identity), respectively. Only these two Rasner Möser OTUs and Rasner Möser OTU 6 were also identified by *dsrB* DGGE analysis (Table S7).

DISCUSSION

Microorganisms carrying novel *dsrAB* types are part of the core microbial community in the Schlöppnerbrunnen II fen and show a distinct depth distribution. FGA analyses revealed the presence of a stable community of *dsrAB*-containing microorganisms over a sampling period of 6 years, showing that members of several novel *dsrAB* lineages and *Syntrophobacter*-related microorganisms are a persistent part of the autochthonous community in the Schlöppnerbrunnen II fen. In each of the analyzed years, clear differences over a depth gradient of 40 cm were evident in FGA hybridization patterns, with only very few probe-target groups being detected in the uppermost, mainly oxic fen soil layer (Fig. 2). Consistent with this observation, qPCR-quantified *dsrA* copy numbers of novel *dsrAB* OTUs 1 and 2 as well as of *Syntrophobacter wolinii*-related OTU 6 were always considerably lower in the uppermost soil layer than in the deeper soil layers. It is unlikely that these depth-dependent differences in the community composition of *dsrAB*-containing microorganisms are influenced by soil water pH, which is relatively constant (pH 4.3 to 4.8) between 0- and 40-cm depths at this fen (44, 68, 69). In peatlands, the position of the water table usually marks the transition between the oxic and anoxic zones. In the Schlöppnerbrunnen II fen, the water table varies over the year, on average between depths of 5 and 30 cm (41, 68), dividing the analyzed depth gradient of 40 cm into three major zones: (i) the uppermost mainly oxygenated 5 cm, (ii) a transition zone of 5 to 30 cm with periodically changing oxic-anoxic conditions, and (iii) the zone below 30 cm, which is anoxic down to the groundwater table (100- to 200-cm depth) (3). While generally regarded as anaerobic microorganisms, it is well known that some SRM (i) can be highly active in oxic-anoxic transition zones and even in oxic environments

FIG. 4. DsrAB consensus tree showing the affiliation of selected *dsrAB* and *dsrA* clone sequences in comparison to *dsrB* DGGE sequences recovered from nine different wetlands: five fens (F), three bogs (B), and a wet meadow (WM). OTUs from the Rasner Möser fen and selected OTUs from the Schlöppnerbrunnen fen sites (51) were based on DsrAB sequences longer than 500 amino acids and are depicted in boldface and colored type. For each Rasner Möser OTU, a representative clone and the number of sequenced clones are given in parentheses and square brackets, respectively. DsrA sequences were added by using the ARB parsimony interactive tool without changing the overall tree topology and are indicated by dotted branches. Phylogenetic positions of DsrB DGGE sequences are indicated by asterisks (numbers behind asterisks indicate the *dsrB* OTU numbers) and were determined by adding the sequences to a separate DsrAB consensus tree using the ARB parsimony interactive tool. In addition, the presence or absence of each *dsrB* OTU in the nine wetlands was inferred from comparisons of DGGE banding patterns and is indicated by the presence or absence of the respective colored square. The scale bar indicates 10% estimated sequence divergence (distance matrix analysis).

(57, 58, 77) and (ii) are able to detoxify, or in some cases even to respire, oxygen in pure culture (11, 20, 47, 74). Just like methanogens and homoacetogens (35, 78), SRM require a low redox potential for growth but have been shown in pure culture to actively establish an oxic-anoxic interface and maintain stable growth bands below this transition zone as long as reductants were present (11). However, growth inhibition due to prolonged exposure to oxygen could restrict the abundance of anaerobic, *dsrAB*-containing microorganisms in the uppermost fen soil layer (0 to 5 cm) on a long-term scale. In contrast, there is evidence that periodic oxidation of the 5- to 30-cm zone, as driven by recurring events of drought and precipitation, stimulates SRM rather than inhibiting growth. This has been observed by ^{35}S radiotracer studies of the Schlöppnerbrunnen II fen site measuring sulfate reduction rates after artificial water table manipulations *in situ* and in controlled mesocosms. Here, sulfate reduction rates reached up to 1,200 nmol cm^{-3} day^{-1}, which can be explained by the reoxidation of reduced sulfur species during oxic periods and the parallel occurrence of water-saturated, anoxic microniches (14, 40, 41). Despite the low sulfate concentration, sulfate reduction is an ongoing process in the anoxic zone, as evident from ^{35}S radiotracer measurements (40, 41). Experimental evidence is accumulating that the rapid anoxic recycling of sulfate is mediated by the oxidation of sulfide mainly by quinone moieties of the large pool of humic matter in peatlands (5, 27, 28, 34) and/or by electric currents spanning from the anoxic zone to the oxic zone, as was shown previously for marine sediments (61). Assuming that the microorganisms detected by their *dsrAB* genes are SRM, these findings could provide an explanation for our observation that there is a temporally stable community of different *dsrAB*-carrying microorganisms below the uppermost soil layer, despite the well-known variations in environmental conditions in this system.

Interestingly, FGA and qPCR analyses both indicated that members of novel *dsrAB* lineages (e.g., OTUs 1, 2, 3, 4, 11, and 14) outnumbered members of lineages that contain cultivated microorganisms. In particular, all soil fractions contained a higher copy number of *dsrA* from the novel OTUs 1 and 2 than from the *Syntrophobacter wolinii*-related OTU 6. In some soil samples from depths of 10 to 30 cm, members of OTUs 1 and 2 even accounted for a significant proportion of the total microbial community (1% to 1.7% of the *dsrA* copy number relative to the total number of bacterial and archaeal 16S rRNA genes) (Fig. 3). These relatively high abundances of ≥0.1% to 1% imply that unknown OTU 1 and OTU 2 members are so-called "core" microorganisms (65) and actively contribute, at least occasionally, to the prevalent biogeochemical processes in the fen.

Novel *dsrAB*-carrying microorganisms are widespread in wetlands. DGGE analyses of nine wetlands with geographical distances ranging from 1 km to 400 km showed that many of the *dsrAB*-containing microorganisms (six OTUs) found in the Schlöppnerbrunnen fens are not endemic but also inhabit other peatlands. Previous molecular fingerprinting studies of anthropogenically impacted sediments (66) and river floodplains (56) reported signatures of biogeography in *dsrAB* data, and the overall *dsrB* DGGE banding pattern also indicated that the spatial distribution of *dsrAB*-containing microorganisms between the nine wetland sites is nonrandom. Being aware that *dsrB* DGGE analysis with degenerate primers is prone to certain biases (7, 60, 62) and restricted by its detection limit, we nevertheless sought to identify environmental and/or geographic factors that govern the biogeography of *dsrAB*-containing microorganisms in wetlands. Spatial variations in microbial community composition can generally depend on contemporary environmental factors, on past events (such as dispersal limitation and past environmental conditions) that lead to genetic differentiation and possibly speciation, or on both (55). If community structure is influenced only by the currently prevailing environmental parameters, otherwise known as the Baas-Becking hypothesis that "everything is everywhere, but the environment selects" (15), we would expect no geographical distance-dependent differences. Indeed, the geographical distance between sites was found to be a poor predictor of the *dsrB* DGGE banding pattern distribution, suggesting that the current biogeography of *dsrAB*-containing microorganisms in wetlands is not a legacy of historical events (55). Although only few environmental parameters (see Table S1 in the supplemental material) were measured, the observed biogeography pattern significantly reflected the influence of environmental variations. In particular, soil pH was the dominant factor that determined the community structure. This finding is consistent with results of a previous general study of the bacterial biogeography in soils, where bacterial richness, diversity, and overall community composition were found to be influenced mainly by soil pH (19). In our study, the *dsrAB*-containing communities in the wetlands seemed to be additionally impacted by the source of water, as bogs, which are fed by precipitation, clustered together in principal component analyses (Fig. 1B). The type of water source can be regarded as a proxy for the nutrient content of peatlands (8, 42). Therefore, microorganisms inhabiting precipitation-dependent bogs generally have to cope with a lower availability of minerals and nutrients than do microorganisms that live in fens, which receive additional substrates by the groundwater flow. Phylogenetic analyses of *dsrB* DGGE bands and a *dsrAB* clone library from the Rasner Möser fen revealed 10 OTUs that were broadly distributed among different bogs and fens; these OTUs include the *Syntrophobacter wolinii*-related OTU and nine OTUs with no closely related cultivated relatives. However, none of these more widely distributed OTUs was found at all sites of a particular wetland type, and thus, general indicator OTUs for bogs or fens were not revealed by our analyses (Fig. 4). The numerical abundance at the long-term experimental peatland field site and broad distribution among peatlands that are located up to several hundred kilometers apart clearly suggest that these novel *dsrAB*-carrying microorganisms have a considerable impact on peatland ecosystem functioning. It has thus far proved challenging to reveal the identity and physiological features of these mysterious microbes (67). However, the relatively high abundance of these as-yet-unidentified microorganisms at a given time and soil depth in the investigated model peatland holds much promise for future research, because it should make them amenable to techniques that allow sorting and genomic or physiological analyses of individual microbial cells (75, 83, 88).

ACKNOWLEDGMENTS

We thank Stephan Duller for help with the development of qPCR assays, Achim Schmalenberger for providing *dsrAB* clones for microarray evaluation, Christina Kaiser for ion chromatographic determination of anion concentrations, and David Berry for revising the manuscript. We are grateful to Jen How Huang, Janine Franke, Alexandra Hamberger, Marco Reiche, and Florian Wenter for their help with sampling.

This research was financially supported by the Austrian Science Fund (grants P18836-B17 and P20185-B17 [A.L.]), the Alexander von Humboldt Foundation (M.P.), the German Federal Ministry of Science and Education (BIOLOG/BIOTA project 01LC0621D [M.W. and A.L.]), the Austrian Federal Ministry of Science and Research (ASEA-UNINET [P.D.]), and the University of Vienna (P.D.).

REFERENCES

1. **Alewell, C., B. Manderscheid, H. Meesenburg, and J. Bittersohl.** 2000. Is acidification still an ecological threat? Nature **407:**856–858.
2. **Alewell, C., and M. Novak.** 2001. Spotting zones of dissimilatory sulfate reduction in a forested catchment: the 34S-35S approach. Environ. Pollut. **112:**369–377.
3. **Alewell, C., S. Paul, G. Lischeid, K. Küsel, and M. Gehre.** 2006. Characterizing the redox status in three different forested wetlands with geochemical data. Environ. Sci. Technol. **40:**7609–7615.
4. **Alewell, C., S. Paul, G. Lischeid, and F. R. Storck.** 2008. Co-regulation of redox processes in freshwater wetlands as a function of organic matter availability? Sci. Total Environ. **404:**335–342.
5. **Blodau, C., B. Mayer, S. Peiffer, and T. R. Moore.** 2007. Support for an anaerobic sulfur cycle in two Canadian peatland soils. J. Geophys. Res. **112:**G02004.
6. **Bodrossy, L., et al.** 2003. Development and validation of a diagnostic microbial microarray for methanotrophs. Environ. Microbiol. **5:**566–582.
7. **Boon, N., W. Windt, W. Verstraete, and E. M. Top.** 2002. Evaluation of nested PCR-DGGE (denaturing gradient gel electrophoresis) with group-specific 16S rRNA primers for the analysis of bacterial communities from different wastewater treatment plants. FEMS Microbiol. Ecol. **39:**101–112.
8. **Bridgham, S. D., J. Pastor, J. A. Janssens, C. Chapin, and T. J. Malterer.** 1996. Multiple limiting gradients in peatlands: a call for a new paradigm. Wetlands **16:**45–65.
9. **Brody, J. P., B. A. Williams, B. J. Wold, and S. R. Quake.** 2002. Significance and statistical errors in the analysis of DNA microarray data. Proc. Natl. Acad. Sci. U. S. A. **99:**12975–12978.
10. **Clarke K. R., and R. N. Gorley.** 2001. PRIMER v5: user manual/tutorial. PRIMER-E, Plymouth, United Kingdom.
11. **Cypionka, H.** 2000. Oxygen respiration by *Desulfovibrio* species. Annu. Rev. Microbiol. **54:**827–848.
12. **D'Aquila, R. T., et al.** 1991. Maximizing sensitivity and specificity of PCR by pre-amplification heating. Nucleic Acids Res. **19:**3749.
13. **Davidson, E. A., and I. A. Janssens.** 2006. Temperature sensitivity of soil carbon decomposition and feedbacks to climate change. Nature **440:**165–173.
14. **Deppe, M., D. M. McKnight, and C. Blodau.** 2010. Effects of short-term drying and irrigation on electron flow in mesocosms of a northern bog and an alpine fen. Environ. Sci. Technol. **44:**80–86.
15. **de Wit, R., and T. Bouvier.** 2006. 'Everything is everywhere, but, the environment selects'; what did Baas Becking and Beijerinck really say? Environ. Microbiol. **8:**755–758.
16. **Dhillon, A., A. Teske, J. Dillon, D. A. Stahl, and M. L. Sogin.** 2003. Molecular characterization of sulfate-reducing bacteria in the Guaymas Basin. Appl. Environ. Microbiol. **69:**2765–2772.
17. **Dise, N. B.** 2009. Peatland response to global change. Science **326:**810–811.
18. **Dowrick, D. J., C. Freeman, M. A. Lock, and B. Reynolds.** 2006. Sulphate reduction and the suppression of peatland methane emissions following summer drought. Geoderma **132:**384–390.
19. **Fierer, N., and R. B. Jackson.** 2006. The diversity and biogeography of soil bacterial communities. Proc. Natl. Acad. Sci. U. S. A. **103:**626–631.
20. **Finster, K. W., and K. U. Kjeldsen.** 2010. Desulfovibrio oceani subsp. oceani sp. nov., subsp. nov. and Desulfovibrio oceani subsp. galateae subsp. nov., novel sulfate-reducing bacteria isolated from the oxygen minimum zone off the coast of Peru. Antonie Van Leeuwenhoek **97:**221–229.
21. **Frolking, S., and N. T. Roulet.** 2007. Holocene radiative forcing impact of northern peatland carbon accumulation and methane emissions. Global Change Biol. **13:**1079–1088.
22. **Gauci, V., et al.** 2004. Sulfur pollution suppression of the wetland methane source in the 20th and 21st centuries. Proc. Natl. Acad. Sci. U. S. A. **101:**12583–12587.
23. **Geets, J., et al.** 2006. DsrB gene-based DGGE for community and diversity surveys of sulfate-reducing bacteria. J. Microbiol. Methods **66:**194–205.
24. **Good, I. J.** 1953. The population frequency of species and the estimation of population parameters. Biometrika **40:**237–264.
25. **Hamberger, A., M. A. Horn, M. G. Dumont, J. C. Murrell, and H. L. Drake.** 2008. Anaerobic consumers of monosaccharides in a moderately acidic fen. Appl. Environ. Microbiol. **74:**3112–3120.
26. **He, Z., et al.** 2007. GeoChip: a comprehensive microarray for investigating biogeochemical, ecological and environmental processes. ISME J. **1:**67–77.
27. **Heitmann, T., and C. Blodau.** 2006. Oxidation and incorporation of hydrogen sulfide by dissolved organic matter. Chem. Geol. **235:**12–20.
28. **Heitmann, T., T. Goldhammer, J. Beer, and C. Blodau.** 2007. Electron transfer of dissolved organic matter and its potential significance for anaerobic respiration in a northern bog. Global Change Biol. **13:**1771–1785.
29. **Horn, M. A., C. Matthies, K. Küsel, A. Schramm, and H. L. Drake.** 2003. Hydrogenotrophic methanogenesis by moderately acid-tolerant methanogens of a methane-emitting acidic peat. Appl. Environ. Microbiol. **69:**74–83.
30. **Houweling, S., T. Kaminski, F. Dentener, J. Lelieveld, and M. Heimann.** 1999. Inverse modeling of methane sources and sinks using the adjoint of a global transport model. J. Geophys. Res. Atmos. **104:**26137–26160.
31. **Huber, E., et al.** 2007. Shift in soil-plant nitrogen dynamics of an alpine-nival ecotone. Plant Soil **301:**65–76.
32. **Imachi, H., et al.** 2006. Non-sulfate-reducing, syntrophic bacteria affiliated with *Desulfotomaculum* cluster I are widely distributed in methanogenic environments. Appl. Environ. Microbiol. **72:**2080–2091.
33. **Joachimiak, M. P., J. L. Weisman, and B. May.** 2006. JColorGrid: software for the visualization of biological measurements. BMC Bioinformatics **7:**225.
34. **Jørgensen, B. B.** 1990. A thiosulfate shunt in the sulfur cycle of marine sediments. Science **249:**152–154.
35. **Karnholz, A., K. Kusel, A. Gossner, A. Schramm, and H. L. Drake.** 2002. Tolerance and metabolic response of acetogenic bacteria toward oxygen. Appl. Environ. Microbiol. **68:**1005–1009.
36. **Keller, J. K., and S. D. Bridgham.** 2007. Pathways of anaerobic carbon cycling across an ombrotrophic-minerotrophic peatland gradient. Limnol. Oceanogr. **52:**96–107.
37. **Kibbe, W. A.** 2007. OligoCalc: an online oligonucleotide properties calculator. Nucleic Acids Res. **35:**W43–W46.
38. **Kjeldsen, K. U., et al.** 2007. Diversity of sulfate-reducing bacteria from an extreme hypersaline sediment, Great Salt Lake (Utah). FEMS Microbiol. Ecol. **60:**287–298.
39. **Klemm, O., and H. Lange.** 1999. Trends of air pollution in the Fichtelgebirge Mountains, Bavaria. Environ. Sci. Pollut. Res. Int. **6:**193–199.
40. **Knorr, K. H., and C. Blodau.** 2009. Impact of experimental drought and rewetting on redox transformations and methanogenesis in mesocosms of a northern fen soil. Soil Biol. Biochem. **41:**1187–1198.
41. **Knorr, K. H., G. Lischeid, and C. Blodau.** 2009. Dynamics of redox processes in a minerotrophic fen exposed to a water table manipulation. Geoderma **153:**379–392.
42. **Koerselman, W., M. B. Van Kerkhoven, and J. T. Verhoeven.** 1993. Release of inorganic N, P and K in peat soils; effect of temperature, water chemistry and water level. Biogeochemistry **20:**63–81.
43. **Koretsky, C. M., et al.** 2007. Spatial variation of redox and trace metal geochemistry in a minerotrophic fen. Biogeochemistry **86:**33–62.
44. **Küsel, K., M. Blothe, D. Schulz, M. Reiche, and H. L. Drake.** 2008. Microbial reduction of iron and porewater biogeochemistry in acidic peatlands. Biogeosciences **5:**1537–1549.
45. **Laue, H., M. Friedrich, J. Ruff, and A. M. Cook.** 2001. Dissimilatory sulfite reductase (desulfoviridin) of the taurine-degrading, non-sulfate-reducing bacterium *Bilophila wadsworthia* RZATAU contains a fused DsrB-DsrD subunit. J. Bacteriol. **183:**1727–1733.
46. **Leloup, J., et al.** 2007. Diversity and abundance of sulfate-reducing microorganisms in the sulfate and methane zones of a marine sediment, Black Sea. Environ. Microbiol. **9:**131–142.
47. **Lemos, R. S., et al.** 2001. The 'strict' anaerobe Desulfovibrio gigas contains a membrane-bound oxygen-reducing respiratory chain. FEBS Lett. **496:**40–43.
48. **Loy, A., et al.** 2008. probeCheck—a central resource for evaluating oligonucleotide probe coverage and specificity. Environ. Microbiol. **10:**2894–2898.
49. **Loy, A., and L. Bodrossy.** 2006. Highly parallel microbial diagnostics using oligonucleotide microarrays. Clin. Chim. Acta **363:**106–119.
50. **Loy, A., et al.** 2009. Reverse dissimilatory sulfite reductase as phylogenetic marker for a subgroup of sulfur-oxidizing prokaryotes. Environ. Microbiol. **11:**289–299.
51. **Loy, A., K. Küsel, A. Lehner, H. L. Drake, and M. Wagner.** 2004. Microarray and functional gene analyses of sulfate-reducing prokaryotes in low-sulfate, acidic fens reveal cooccurrence of recognized genera and novel lineages. Appl. Environ. Microbiol. **70:**6998–7009.
52. **Loy, A., et al.** 2002. Oligonucleotide microarray for 16S rRNA gene-based detection of all recognized lineages of sulfate-reducing prokaryotes in the environment. Appl. Environ. Microbiol. **68:**5064–5081.
53. **Ludwig, W., et al.** 2004. ARB: a software environment for sequence data. Nucleic Acids Res. **32:**1363–1371.
54. **Markham, N. R., and M. Zuker.** 2005. DINAMelt Web server for nucleic acid melting prediction. Nucleic Acids Res. **33:**W577–W581.

55. **Martiny, J. B., et al.** 2006. Microbial biogeography: putting microorganisms on the map. Nat. Rev. Microbiol. **4:**102–112.
56. **Miletto, M., et al.** 2008. Biogeography of sulfate-reducing prokaryotes in river floodplains. FEMS Microbiol. Ecol. **64:**395–406.
57. **Minz, D., et al.** 1999. Unexpected population distribution in a microbial mat community: sulfate-reducing bacteria localized to the highly oxic chemocline in contrast to a eukaryotic preference for anoxia. Appl. Environ. Microbiol. **65:**4659–4665.
58. **Mussmann, M., K. Ishii, R. Rabus, and R. Amann.** 2005. Diversity and vertical distribution of cultured and uncultured Deltaproteobacteria in an intertidal mud flat of the Wadden Sea. Environ. Microbiol. **7:**405–418.
59. **Muyzer, G., E. C. de Waal, and A. G. Uitterlinden.** 1993. Profiling of complex microbial populations by denaturing gradient gel electrophoresis analysis of polymerase chain reaction-amplified genes coding for 16S rRNA. Appl. Environ. Microbiol. **59:**695–700.
60. **Nicolaisen, M. H., and N. B. Ramsing.** 2002. Denaturing gradient gel electrophoresis (DGGE) approaches to study the diversity of ammonia-oxidizing bacteria. J. Microbiol. Methods **50:**189–203.
61. **Nielsen, L. P., N. Risgaard-Petersen, H. Fossing, P. B. Christensen, and M. Sayama.** 2010. Electric currents couple spatially separated biogeochemical processes in marine sediment. Nature **463:**1071–1074.
62. **Nikolausz, M., R. Sipos, S. Revesz, A. Szekely, and K. Marialigeti.** 2005. Observation of bias associated with re-amplification of DNA isolated from denaturing gradient gels. FEMS Microbiol. Lett. **244:**385–390.
63. **Palmer, K., H. L. Drake, and M. A. Horn.** 2010. Association of novel and highly diverse acid-tolerant denitrifiers with N_2O fluxes of an acidic fen. Appl. Environ. Microbiol. **76:**1125–1134.
64. **Paul, S., K. Kusel, and C. Alewell.** 2006. Reduction processes in forest wetlands: tracking down heterogeneity of source/sink functions with a combination of methods. Soil Biol. Biochem. **38:**1028–1039.
65. **Pedros-Alio, C.** 2006. Marine microbial diversity: can it be determined? Trends Microbiol. **14:**257–263.
66. **Perez-Jimenez, J. R., and L. J. Kerkhof.** 2005. Phylogeography of sulfate-reducing bacteria among disturbed sediments, disclosed by analysis of the dissimilatory sulfite reductase genes (dsrAB). Appl. Environ. Microbiol. **71:**1004–1011.
67. **Pester, M., N. Bittner, P. Deevong, M. Wagner, and A. Loy.** 2010. A 'rare biosphere' microorganism contributes to sulfate reduction in a peatland. ISME J. **4:**1591–1602.
68. **Reiche, M., A. Hädrich, G. Lischeid, and K. Küsel.** 2009. Impact of manipulated drought and heavy rainfall events on peat mineralization processes and source-sink functions of an acidic fen. J. Geophys. Res. **114:**G02021.
69. **Reiche, M., G. Torburg, and K. Küsel.** 2008. Competition of Fe(III) reduction and methanogenesis in an acidic fen. FEMS Microbiol. Ecol. **65:**88–101.
70. **Rozen, S., and H. Skaletsky.** 2000. Primer3 on the WWW for general users and for biologist programmers. Methods Mol. Biol. **132:**365–386.
71. **Sanguin, H., et al.** 2006. Development and validation of a prototype 16S rRNA-based taxonomic microarray for Alphaproteobacteria. Environ. Microbiol. **8:**289–307.
72. **Schloss, P. D., and J. Handelsman.** 2005. Introducing DOTUR, a computer program for defining operational taxonomic units and estimating species richness. Appl. Environ. Microbiol. **71:**1501–1506.
73. **Schmalenberger, A., H. L. Drake, and K. Küsel.** 2007. High unique diversity of sulfate-reducing prokaryotes characterized in a depth gradient in an acidic fen. Environ. Microbiol. **9:**1317–1328.
74. **Sigalevich, P., M. V. Baev, A. Teske, and Y. Cohen.** 2000. Sulfate reduction and possible aerobic metabolism of the sulfate-reducing bacterium Desulfovibrio oxyclinae in a chemostat coculture with Marinobacter sp. strain MB under exposure to increasing oxygen concentrations. Appl. Environ. Microbiol. **66:**5013–5018.
75. **Stepanauskas, R., and M. E. Sieracki.** 2007. Matching phylogeny and metabolism in the uncultured marine bacteria, one cell at a time. Proc. Natl. Acad. Sci. U. S. A. **104:**9052–9057.
76. **ter Braak, C. J. F., and P. Šmilauer.** 2002. CANOCO reference manual and CanoDraw for Windows user's guide: software for canonical community ordination (version 4.5). Microcomputer Power, Ithaca, NY.
77. **Teske, A., et al.** 1998. Sulfate-reducing bacteria and their activities in cyanobacterial mats of Solar Lake (Sinai, Egypt). Appl. Environ. Microbiol. **64:**2943–2951.
78. **Tholen, A., M. Pester, and A. Brune.** 2007. Simultaneous methanogenesis and oxygen reduction by *Methanobrevibacter cuticularis* at low oxygen fluxes. FEMS Microbiol. Ecol. **62:**303–312.
79. **Turunen, J., E. Tomppo, K. Tolonen, and A. Reinikainen.** 2002. Estimating carbon accumulation rates of undrained mires in Finland—application to boreal and subarctic regions. Holocene **12:**69–80.
80. **van Hijum, S. A. F. T., et al.** 2005. A generally applicable validation scheme for the assessment of factors involved in reproducibility and quality of DNA-microarray data. BMC Genomics **6:**77.
81. **Vile, M. A., S. D. Bridgham, and R. K. Wieder.** 2003. Response of anaerobic carbon mineralization rates to sulfate amendments in a boreal peatland. Ecol. Appl. **13:**720–734.
82. **Vile, M. A., S. D. Bridgham, R. K. Wieder, and M. Novak.** 2003. Atmospheric sulfur deposition alters pathways of gaseous carbon production in peatlands. Global Biogeochem. Cycles **17:**27.1–27.7.
83. **Wagner, M.** 2009. Single-cell ecophysiology of microbes as revealed by Raman microspectroscopy or secondary ion mass spectrometry imaging. Annu. Rev. Microbiol. **63:**411–429.
84. **Wagner, M., et al.** 2005. Functional marker genes for identification of sulfate-reducing prokaryotes. Methods Enzymol. **397:**469–489.
85. **Wagner, M., H. Smidt, A. Loy, and J. Zhou.** 2007. Unravelling microbial communities with DNA microarrays: challenges and future directions. Microb. Ecol. **53:**498–506.
86. **Wind, T., and R. Conrad.** 1997. Localization of sulfate reduction in planted and unplanted rice field soil. Biogeochemistry **37:**253–278.
87. **Wuebbles, D. J., and K. Hayhoe.** 2002. Atmospheric methane and global change. Earth Sci. Rev. **57:**177–210.
88. **Xie, C., D. Chen, and Y. Q. Li.** 2005. Raman sorting and identification of single living micro-organisms with optical tweezers. Opt. Lett. **30:**1800–1802.
89. **Zverlov, V., et al.** 2005. Lateral gene transfer of dissimilatory (bi)sulfite reductase revisited. J. Bacteriol. **187:**2203–2208.